

Regional impacts poorly constrained by climate sensitivity

Article

Published Version

Creative Commons: Attribution 4.0 (CC-BY)

Open Access

Swaminathan, R. ORCID: <https://orcid.org/0000-0001-5853-2673>, Schewe, J., Walton, J., Zimmermann, K., Jones, C., Betts, R., Burton, C., Jones, C., Mengel, M., Reyer, C., Turner, A. ORCID: <https://orcid.org/0000-0002-0642-6876> and Weigel, K. (2024) Regional impacts poorly constrained by climate sensitivity. *Earth's Future*, 12 (12). e2024EF004901. ISSN 2328-4277 doi: 10.1029/2024EF004901 Available at <https://centaur.reading.ac.uk/119178/>

It is advisable to refer to the publisher's version if you intend to cite from the work. See [Guidance on citing](#).

To link to this article DOI: <http://dx.doi.org/10.1029/2024EF004901>

Publisher: Wiley

All outputs in CentAUR are protected by Intellectual Property Rights law, including copyright law. Copyright and IPR is retained by the creators or other copyright holders. Terms and conditions for use of this material are defined in the [End User Agreement](#).

www.reading.ac.uk/centaur

CentAUR

Central Archive at the University of Reading

Reading's research outputs online

Earth's Future

RESEARCH ARTICLE

10.1029/2024EF004901

Ranjini Swaminathan and Jacob Schewe contributed equally to this work.

Key Points:

- Future changes in climatic drivers of floods, droughts, and wildfires are generally not correlated with climate sensitivity in Sixth Coupled Model Intercomparison Project models
- Model selection for impacts solely based on climate sensitivity is not justified and may lead to an underestimation of climate risks
- Model internal variability plays an important role in future projections of climate impact drivers

Supporting Information:

Supporting Information may be found in the online version of this article.

Correspondence to:

R. Swaminathan,
r.swaminathan@reading.ac.uk

Citation:

Swaminathan, R., Schewe, J., Walton, J., Zimmermann, K., Jones, C., Betts, R. A., et al. (2024). Regional impacts poorly constrained by climate sensitivity. *Earth's Future*, 12, e2024EF004901. <https://doi.org/10.1029/2024EF004901>

Received 17 MAY 2024

Accepted 27 OCT 2024

Author Contributions:

Conceptualization: Jacob Schewe, Colin Jones, Richard A. Betts, Chris D. Jones, Matthias Mengel, Christopher P. O. Reyer

Data curation: Ranjini Swaminathan, Jeremy Walton, Klaus Zimmermann, Katja Weigel

Formal analysis: Ranjini Swaminathan, Jacob Schewe, Jeremy Walton, Klaus Zimmermann, Colin Jones, Richard A. Betts, Chantelle Burton, Chris D. Jones, Matthias Mengel, Christopher P. O. Reyer, Andrew G. Turner, Katja Weigel

Investigation: Ranjini Swaminathan, Jacob Schewe, Jeremy Walton,

© 2024. The Author(s).

This is an open access article under the terms of the [Creative Commons](#)

Attribution License, which permits use, distribution and reproduction in any medium, provided the original work is properly cited.

Regional Impacts Poorly Constrained by Climate Sensitivity



Ranjini Swaminathan¹ , Jacob Schewe² , Jeremy Walton³ , Klaus Zimmermann⁴, Colin Jones⁵, Richard A. Betts^{3,6} , Chantelle Burton³ , Chris D. Jones^{3,7} , Matthias Mengel² , Christopher P. O. Reyer² , Andrew G. Turner⁸, and Katja Weigel^{9,10}

¹Department of Meteorology and National Centre for Earth Observation, University of Reading, Reading, UK, ²Potsdam Institute for Climate Impact Research, Member of the Leibniz Association, Potsdam, Germany, ³Met Office Hadley Centre for Climate Science and Services, Exeter, UK, ⁴Swedish Meteorological and Hydrological Institute, Rossby Centre, Norrköping, Sweden, ⁵National Centre for Atmospheric Science and School of Earth and Environment, University of Leeds, Leeds, UK, ⁶Global Systems Institute, University of Exeter, Exeter, UK, ⁷School of Geographical Science, University of Bristol, Bristol, UK, ⁸National Centre for Atmospheric Science and Department of Meteorology, University of Reading, Reading, UK, ⁹University of Bremen, Institute of Environmental Physics (IUP), Bremen, Germany, ¹⁰Deutsches Zentrum für Luft- und Raumfahrt (DLR), Institut für Physik der Atmosphäre, Oberpfaffenhofen, Germany

Abstract Climate risk assessments must account for a wide range of possible futures, so scientists often use simulations made by numerous global climate models to explore potential changes in regional climates and their impacts. Some of the latest-generation models have high effective climate sensitivities (EffCS). It has been argued these “hot” models are unrealistic and should therefore be excluded from analyses of climate change impacts. Whether this would improve regional impact assessments, or make them worse, is unclear. Here we show there is no universal relationship between EffCS and projected changes in a number of important climatic drivers of regional impacts. Analyzing heavy rainfall events, meteorological drought, and fire weather in different regions, we find little or no significant correlation with EffCS for most regions and climatic drivers. Even when a correlation is found, internal variability and processes unrelated to EffCS have similar effects on projected changes in the climatic drivers as EffCS. Model selection based solely on EffCS appears to be unjustified and may neglect realistic impacts, leading to an underestimation of climate risks.

Plain Language Summary Climate impact researchers often must decide which of the many available global climate models to use for their analyses. It has been suggested models with very high climate sensitivities should be excluded from impact analyses, because their global mean temperature projections are unrealistic. However, we show that projected future changes in climatic drivers of floods, droughts, and wildfires, across many regions of the world, are not correlated with model climate sensitivity. Regional impacts depend on numerous processes and phenomena many of which are unrelated to climate sensitivity. Excluding models solely on the basis of their climate sensitivity is thus not justified, and can lead to important impacts being ignored by policymakers, with serious consequences for society.

1. Introduction

The use of climate projections for impact assessment often exploits numerous climate and Earth system models (ESMs). The Coupled Model Intercomparison Project (Veronika Eyring et al., 2016) (CMIP) provides underpinning simulations to the Intergovernmental Panel on Climate Change (IPCC) analysis of climate projections (Lee et al., 2021), changes in climate impact drivers (Ranasinghe et al., 2021), and assessment of impacts and vulnerability (IPCC, 2022). Using a diverse set of ESMs, the CMIP ensemble aims to span the uncertainty range of future projections, including potential high impact, low-likelihood events (Wood et al., 2023). It is important that CMIP models represent plausible future evolutions of the climate system and thus perform well against observations (Eyring et al., 2019). A range of studies have shown improvement over generations of models, including from CMIP5 to CMIP6 (Eyring et al., 2021). For instance, compared to CMIP5, biases in temperature, water vapor, and precipitation are significantly reduced in CMIP6 (Bock et al., 2020); and the simulation of wildfires is improved with respect to both total fire activity as well as spatial and temporal patterns (Li et al., 2024). We therefore expect CMIP6 to represent an advance for use in impact studies.

One widely discussed change from CMIP5 to CMIP6 is an increased range in model effective climate sensitivity (effective climate sensitivities (EffCS)) — the near-equilibrium increase in global mean surface temperature due to a doubling in atmospheric CO₂ — with several CMIP6 models having EffCS above the assessed likely and very

Klaus Zimmermann, Colin Jones, Richard A. Betts, Chantelle Burton, Chris D. Jones, Matthias Mengel, Christopher P. O. Reyer, Andrew G. Turner, Katja Weigel

Methodology: Ranjini Swaminathan, Jacob Schewe, Jeremy Walton, Klaus Zimmermann, Colin Jones, Richard A. Betts, Chris D. Jones, Matthias Mengel, Christopher P. O. Reyer, Andrew G. Turner, Katja Weigel

Resources: Ranjini Swaminathan, Jeremy Walton, Klaus Zimmermann, Katja Weigel

Software: Ranjini Swaminathan, Jeremy Walton, Klaus Zimmermann, Matthias Mengel, Katja Weigel

Validation: Ranjini Swaminathan, Jeremy Walton, Klaus Zimmermann, Colin Jones, Richard A. Betts, Chantelle Burton, Matthias Mengel, Christopher P. O. Reyer, Andrew G. Turner, Katja Weigel

Visualization: Ranjini Swaminathan, Jacob Schewe, Jeremy Walton, Klaus Zimmermann, Colin Jones, Chris D. Jones, Matthias Mengel, Christopher P. O. Reyer, Andrew G. Turner, Katja Weigel

Writing – original draft:

Ranjini Swaminathan, Jacob Schewe, Jeremy Walton, Colin Jones, Richard A. Betts, Chantelle Burton, Chris D. Jones, Matthias Mengel, Christopher P. O. Reyer, Andrew G. Turner, Katja Weigel

Writing – review & editing:

Ranjini Swaminathan, Jacob Schewe, Jeremy Walton, Colin Jones, Richard A. Betts, Chantelle Burton, Chris D. Jones, Matthias Mengel, Christopher P. O. Reyer, Andrew G. Turner, Katja Weigel

Writing – review & editing:

Ranjini Swaminathan, Jacob Schewe, Jeremy Walton, Colin Jones, Richard A. Betts, Chantelle Burton, Chris D. Jones, Matthias Mengel, Christopher P. O. Reyer, Andrew G. Turner, Katja Weigel

likely ranges in the IPCC's sixth assessment report (AR6) (Forster et al., 2021). A recent study (Hausfather et al., 2022) suggested such “hot models” warm faster than is realistic, leading to concern that impact studies which draw from the full CMIP6 ensemble could overestimate the impacts of climate change. The IPCC tackled this by constraining projections of global mean temperature based on multiple lines of evidence (Lee et al., 2021). This approach is not yet available for other quantities. Hausfather et al. (2022) recommend filtering out models with EffCS outside the assessed likely range when performing impact assessment over a particular period (as opposed to global warming levels, which may not always be appropriate). While this may be reasonable for global mean surface air temperature, it is less clear what it means for assessments of regional change, and for quantities other than surface temperature. Projections of regional climate change, especially related to hydrological processes, often have a greater range than projections of global mean temperature. While this range is partly related to spread in the magnitude of the warming response to CO₂, changes in circulation patterns and heterogeneous forcings, such as aerosols (Samset et al., 2016) and land-use change (Boysen et al., 2020), also contribute. Furthermore, some studies find high-EffCS models actually perform better than other models when evaluated for certain regions and applications (Palmer et al., 2023; Ribes et al., 2021, 2022).

We explore CMIP6-projected changes in regional climate impact drivers of fire, drought, and monsoon flooding, across a number of important regions, to assess the extent to which projected changes in these drivers are correlated with model EffCS. A regional climate impact driver (Ruane et al., 2022) is a measure of climate known to drive an important societal/environmental impact in the same region; the driver (e.g., extreme monsoon rainfall) can be directly diagnosed from an ESM, while the impact (e.g., flooding) typically cannot. Calculating changes at the end of the century relative to the recent past, following three different Shared Socio–economic Pathway scenarios (Riahi et al., 2017) (see Materials and methods), we find only very few examples of a significant correlation between projected changes in an impact driver and model EffCS. Even for the limited number of cases where a correlation with EffCS is identified, the spread of future change in a given impact driver across a single model ensemble (i.e., solely due to different model initial conditions), or between models with similar EffCS values, is comparable in magnitude to the spread across the full ensemble. This means that internal variability, as well as processes unrelated to EffCS, play at least as large a role as EffCS in determining future changes in our three climate impact drivers. Given the absence of any clear correlation between projected changes in our regional impact drivers and EffCS, we argue it is not justified to filter out ESMs for impact studies solely based on EffCS.

2. Materials and Methods

2.1. Climate Impact Drivers

We use drivers representing three different climate impacts: floods, drought and fire. All three impacts are clearly associated with climate change and expected to worsen under future conditions (Caretta et al., 2022; Parmesan et al., 2022). For each climate impact driver, we identify a measure whose magnitude is expected to be a strong driver of the magnitude of the associated impact, and analyze the change in this measure between a historical period (1995–2014) and a future period (2081–2100). Our main analysis (presented in the main Results section of the paper) is based on SSP3-7.0, a high warming scenario from Tier 1 of the Scenario Model Intercomparison Project (ScenarioMIP) (O'Neill et al., 2016) that can be expected to inform many climate impact studies in the near future; it is part of the current simulation round of the Inter-Sectoral Impact Model Intercomparison Project (ISIMIP, www.isimip.org). To test the robustness of our findings to different assumptions regarding CO₂ emissions, aerosol forcing, and land use change, we repeat our analysis for SSP2-4.5 and SSP5-8.5. These results are shown in detail in Supporting Information S1 and confirm the findings based on the SSP3-7.0 ensemble.

2.1.1. Floods

As a proxy for pluvial flood risk associated with heavy monsoon rainfall, we calculate the area averaged cumulative 5-day rainfall amounts for a given region for the historical and future periods. The difference between the total rainfall amounts of the top 20 such rain events from each period is then calculated as our flood metric.

2.1.2. Drought

Drought is defined as an *anomalous condition* with respect to local and seasonal characteristics, rather than an absolute threshold. We use the Standardized Precipitation Evapotranspiration Index (SPEI) (Beguería et al., 2014; Vicente-Serrano et al., 2010), with the Hargreaves approximation for potential evapotranspiration (Hargreaves & Samani, 1985) (PE) to investigate future change in extreme drought occurrence. SPEI is a widely used metric to characterize atmospheric drought and integrates not only precipitation but also evapotranspiration, meaning that it accounts for the role of temperature in determining the amount of water the atmosphere holds, which is important for our study given that we look at the role of climate sensitivity expressed by temperature.

We follow (Martin, 2018) in the calculation of the number of drought events per year based on SPEI. For each ensemble member we calculate the difference in average number of drought events for each region between the future and historical periods. We use v1.8 of the SPEI.R library (Beguería et al., 2023) to calculate SPEI. Selecting an accumulation period of 6 months, we use a threshold of months with $\text{SPEI} < -2$ to identify extreme droughts. SPEI is calculated by fitting a log-logistic distribution to the difference between precipitation and PE for monthly data. The average SPEI value is 0, which corresponds to a cumulative probability of 50% for this difference, whilst the standard deviation is 1. Following a normal distribution, a threshold of < -2 (two standard deviations lower than the average) will find extreme droughts in 2.3% of all months.

2.1.3. Fire

Wildfires are key drivers of ecosystem dynamics and carbon cycling (Lasslop et al., 2019) and, while overall global burned area is decreasing (Andela et al., 2017), climate change driven increases in frequency and intensity of wildfires have strong effects on human health (Johnston et al., 2021; Pullabhotla et al., 2023) and economic value of land (Wang & Lewis, 2024). We calculate the number of fire-risk days for each period, using the Canadian Fire Weather Index (FWI). The FWI integrates effects of local weather conditions and fuel moisture on fire behavior. It can be calculated from climatic variables alone (temperature, precipitation, relative humidity and wind speed) and, because the different sub-indices can be regionally calibrated, has been widely used across different forest types in the world. Established by (van Wagner, 1987) the FWI has seen some development (Lawson & Armitage, 2008) and is widely used to gauge fire risk. FWI is calculated via a multistep process taking many factors of forest fire risk into account and culminating in a daily index with arbitrary units. These numbers are then typically classified according to chosen thresholds into several classes of risk, such as low, medium, and high; resulting in a risk class for every day at a given point (Lawson & Armitage, 2008). For our purposes of evaluating the impact of climate change as predicted by different climate models, we employ a simplified scheme with a single threshold. We classify all days at a given point with a FWI above that threshold as high fire risk days and count the number of such days in a 20 year period for a given region. By comparing this number for the future period with the historical period, we obtain a measure for the change in fire risk induced by climate-driven changes in weather.

2.2. Choice of Regions

The three climate impact drivers are each evaluated over a set of three (four for flood) regions where the corresponding impact is known to be large and to affect large numbers of people. Regions are further selected to cover different continents and both the tropics and temperate mid-latitudes. For flood, we look at four different regions: Core Indian Monsoon (CIM), Central West African Monsoon (CWAF), North and South Central American Monsoons (NCA and SCA). The CIM region was defined as the area between 18–27 N and 74–88 E; the CWAF to be 7.5–15 N and 10 W–10 E as defined in (Wu et al., 2020) and the NCA and SCA regions as defined in the AR6 WGI Reference Set of Land and Ocean Regions (Iturbide et al., 2020; Speizer et al., 2022). The regions selected for drought are also defined in the AR6 WGI, which are the Mediterranean (MED), considered a climate change hotspot, and East Asia (EAS) and Central North America (CNA), which are agriculturally important regions affected by severe droughts in recent years. For fire, we choose three different regions that are known to suffer from forest fires and that are at high risk from a future increase in this impact, namely Western North America (WNA) as given by the IPCC AR6 regions, the Amazon basin (AMZ), here defined as the combination of two AR6 regions (South-American-Monsoon and Northern South-America), as well as a region of Australia (AUS), again defined by the combination of two AR6 regions (Eastern Australia and Southern Australia).

2.3. Statistical Methods

The measure used to define Earth System Model (ESM) sensitivity in our analysis is the Effective Climate Sensitivity (EffCS) and not the equilibrium climate sensitivity. The true equilibrium climate sensitivity is rarely assessed for ESMs as this requires very long model integrations. EffCS is diagnosed from 150-year abrupt-4xCO₂ experiments following the method of Gregory et al. (2004). It is generally somewhat smaller than the true equilibrium climate sensitivity diagnosed from 2xCO₂ experiments run to equilibrium, mainly due to increasingly positive, temperature-dependent feedbacks activating on very long timescales (Bloch-Johnson et al., 2021). Note that in some studies, “ECS” is used to denote effective climate sensitivity. Here we use EffCS throughout. We use the same EffCS values as (Hausfather et al., 2022), calculated as described by (Zelinka et al., 2020) and consistent with what is reported in Chapter 7 of the Sixth IPCC Assessment Report (Forster et al., 2021).

We establish the relationship between our choice of metric for changes in different regional impacts, such as potential short term flooding events, fire occurrence days or drought indices, and the EffCS of ESMs by calculating a linear fit between the two quantities. In this, we assume that a linear relationship exists between the two quantities. We then determine the statistical significance of this relationship using null hypothesis testing based on the Student's *t*-test for significance at the 95% confidence interval. When considering metrics of ensemble projections from a single model, we use the minimum and maximum ensemble member metric values from models with ensemble sizes larger than one or just the single ensemble member available and calculate lines for all possible combinations of these metric values across models (see Figures 2–4). We then calculate the number of statistically significant lines using null hypothesis testing as before and report results. Hence, we sample the full range of possible metric values.

3. Data

Our study uses a selection of 18 different ESMs from the Sixth CMIP6. Our selection criteria were based on maximizing diversity across models and EffCS values of models. For each model that had the requisite variables for calculating a given metric, we used the first 10 or all available ensemble members (if fewer than 10 were available) to represent the spread due to internal variability. All data was downloaded from Earth System Grid Federation (ESGF) nodes (<https://esgf.llnl.gov/>) and preprocessed using the open source software ESMValTool (<https://esmvaltool.org/>) (Righi et al., 2020). The list of models and ensemble members used in our work is provided in Table 1. The r1 member is always included; this is also the ensemble member that is used in many impact studies relying on single-member multi-model ensembles (Frieler et al., 2017). Not all models had the necessary variables for every climate impact driver, therefore the set of models differs slightly between Figures 2–4.

4. Results

To demonstrate the effect of filtering out “hot models”, we separate the CMIP6 ensemble into two sets: one with EffCS above 4.5K (referred to as high-EffCS hereafter), and another with EffCS below 4.5K (low-med-EffCS hereafter) and plot frequency distributions of the simulated change in each climate impact driver (referred to as metric hereafter), for the two model subsets, for each region of study. We choose this notation because this set includes both low and medium EffCS values, according to the IPCC AR6 assessed range placing the best estimate of EffCS at 3K. Applying such a distinction does not separate the frequency distributions of projected change in our three metrics, with the two distributions largely overlapping for the majority of metrics and regions (Figure 1). In a few cases, the high-EffCS set includes values not projected by any of the low-med-EffCS models, for instance, large increases in high fire weather days in the Amazon region (AMZ), or in total rainfall in Central West Africa (CWAF). Even for these metrics and regions, the overlap between the two distributions is large, suggesting the projected change is not solely decided by EffCS. Moreover, high-EffCS models do not always project larger changes in our metrics; in Western North America (WNA), the high-EffCS set includes more simulations projecting a smaller increase in fire weather than the low-med-EffCS set. Similar conclusions emerge when just looking at the five CMIP6 models selected as core models for the Inter-Sectoral Impact Model Intercomparison project, ISIMIP (Lange & Büchner, 2021) (see stars in Figure 1).

Should the hottest models be filtered out to remove the most extreme projected changes? This would need a solid justification because filtering out particular models can result in vast ranges of potential impacts being excluded.

Table 1

List of Sixth Coupled Model Intercomparison Project Models and Ensemble Members Used for the Three Climate Impact Drivers Under SSP3-7.0, Along With Their Effective Climate Sensitivities Values as Given in (Hausfather et al., 2022)

Model	EffCS	Ensemble members for monsoon impacts	Ensemble members for drought impacts	Ensemble members for fire impacts
ACCESS-ESM1-5	3.88	r1–10 (10 variants)	r1, r2, r4–10 (9 variants)	r1, r2, r4–10 (9 variants)
AWI-CM-1-1MR	3.16		r1	
CESM2-WACCM	4.68	r1		
CMCC-ESM2	3.58	r1	r1	r1
CNRM-ESM2-1	4.79	r1	r1	
CanESM5	5.64	r1–10 (10 variants)	r1–10 (10 variants)	r1–10 (10 variants)
EC-Earth3-AerChem	3.87	r1, r3 (2 variants)	r1, r3 (2 variants)	
FGOALS-g3	2.87	r1, r3–5 (4 variants)	r1, r3–5 (4 variants)	r1, r3–5 (4 variants)
GFDL-ESM4	2.65	r1	r1	r1
INM-CM5-0	1.92	r1–5 (5 variants)	r1–5 (5 variants)	r1–5 (5 variants)
IPSL-CM6A-LR	4.70	r(1–9) (9 variants)	r(1–9) (9 variants)	r(1–9) (9 variants)
KACE-1-0-G	4.75	r1–3 (3 variants)	r1, r2 (2 variants)	r1–3 (3 variants)
MIROC-ES2L	2.66	r1–10 (10 variants)	r1–10 (10 variants)	r1–10 (10 variants)
MPI-ESM1-2-HR	2.98	r(1–10) (10 variants)	r(1–10) (10 variants)	r(1–10) (10 variants)
MRI-ESM2-0	3.13	r1–5 (5 variants)	r1–5 (5 variants)	r1–5 (5 variants)
NorESM2-MM	2.49	r1		r1
TaiESM1	4.36	r1		r1
UKESM1-0-LL	5.36	r(1–4, 8–10) (7 variants)	r(1–4, 8–10) (7 variants)	r(1–4, 8–10) (7 variants)

For instance, in the five-member ISIMIP ensemble, removing the hottest model would ignore the upper half of the low-med CMIP6 spread of the flood metric in the core Indian monsoon (CIM) region, as well as the fire metric in AMZ (cf. red stars in Figure 1). A necessary, though not sufficient, condition for constraining a model ensemble based on EffCS would be a statistically significant, ideally explainable, correlation between the metric (the projected change in the regional climate impact driver) and EffCS. In the following, we investigate whether such a correlation exists for our three metrics. We further assess how the spread in our three metrics, expressed as a function of EffCS, compares with the spread of the same metric for individual model ensembles, independent of EffCS, and across the full CMIP6 ensemble.

Table 2 shows, for each metric, the difference between the median value for the high-EffCS set and the median value for the low-med-EffCS set. It further shows the median and largest spread in each metric across only low-med-EffCS models. In all cases, except AMZ fire, the largest spread in the metric across low-med-EffCS models is bigger than the difference in the median of the metric between high- and low-med-EffCS sets. This is largely still the case when only the median spread in low-med-EffCS models is considered, although for CIM and CWAF, differences between the high- and low-med-EffCS ensembles are comparable to the spread in the low-med-EffCS set. This suggests that internal variability across an individual model or group of models clustered by EffCS, has a larger (or equivalent) influence on the metric than does EffCS. EffCS therefore appears to not be the sole cause of changes in our three selected metrics and thus also in the resultant impacts. We investigate these potential additional controls in the following subsections.

4.1. Flood

We consider projected changes in the 20 most intense, area-average, 5-day precipitation accumulations; a metric indicative of the change in short-term flood risk. Most ensemble members show an increase in this metric over both CIM and CWAF regions, and either little change or a slight reduction over North (NCA) and South Central America (SCA) (Figure 2). This agrees with previous studies (Wang et al., 2020), with an increase in the South Asian and West African monsoons attributed to the northern hemisphere land mass warming more rapidly than adjacent oceans, and more rapidly than the southern hemisphere due to the different land mass distributions

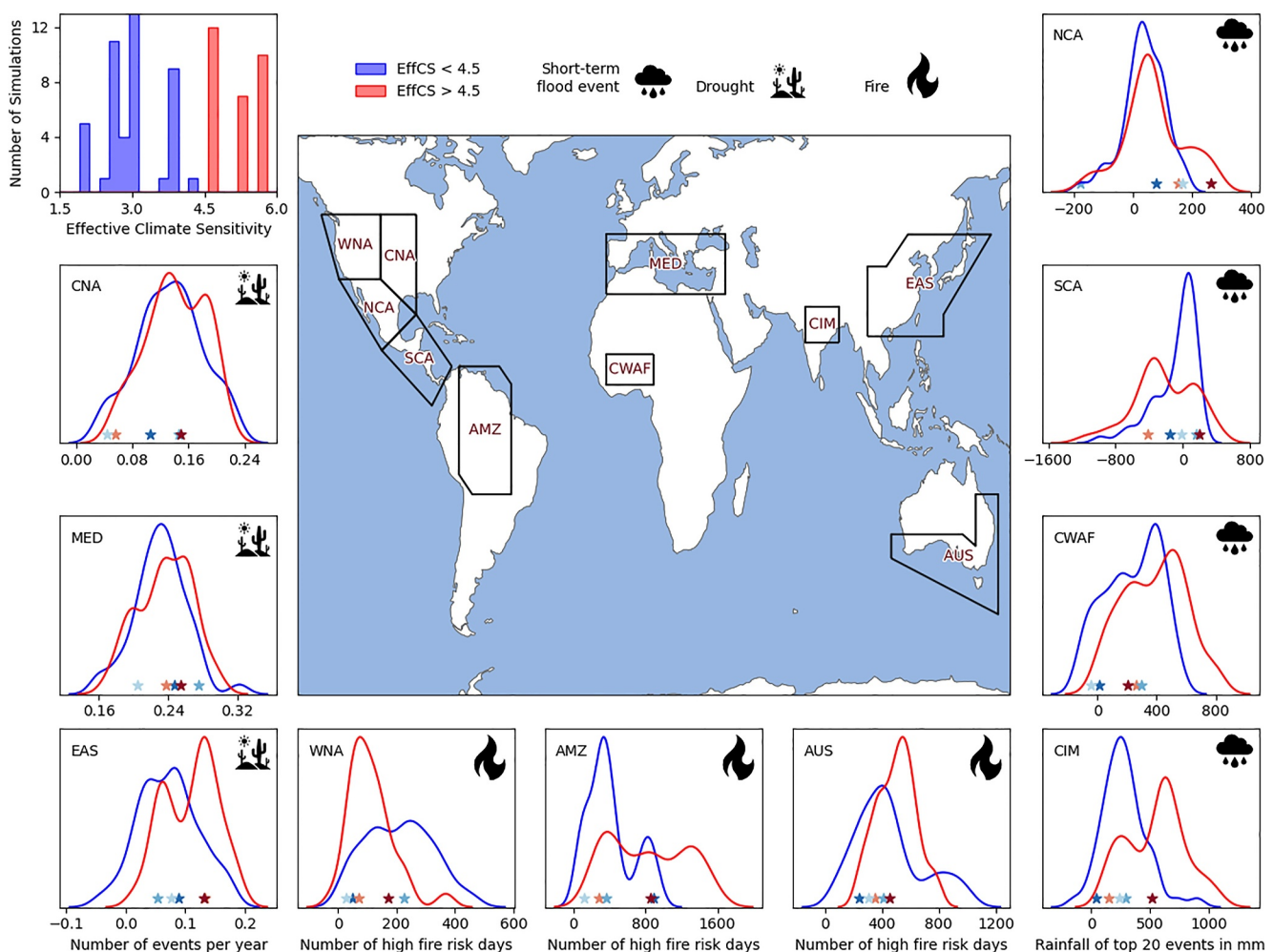


Figure 1. Frequency distribution of projected change in our three regional climate drivers (metrics). Top left: number of model simulations with a given effective climate sensitivities (EffCS) value below (blue) or above (red) 4.5 K. Other panels show the distribution of projected change in the metrics for—drought, left; fire, bottom; monsoon flood, right—for each of the two model subsets (vertical axis shows normalized occurrence, i.e. the area under each curve is equal to 1). The value of 4.5 K is between the upper bounds of the AR6 assessed likely (4 K) and very likely (5 K) ranges for EffCS, and provides for a sufficient number of simulations in each of the subsets. Stars indicate the metric values for five model simulations that are used as input to many impact models (Lange & Büchner, 2021), and are color-coded by EffCS (cf. legend of Figure 2). The map shows the regions over which the impact drivers are analyzed. See Materials and methods section for more detail on how the projected change in each driver was calculated, model simulations, and statistical methods.

(Byrne & O’Gorman, 2018). In addition, atmospheric water vapor increases strongly with warming temperatures (Held & Soden, 2006), increasing the availability of water in northern hemisphere monsoon circulations.

To test the relationship between our monsoon metric and EffCS across the full CMIP6 ensemble, we calculate a linear fit between the two quantities for every possible combination of one member from each model. For CIM, the relationship is positive and statistically significant at the 95% level for the majority (~78%) of combinations, while CWAF shows only ~4% of combinations with a significant correlation (Table 3). Both NCA and SCA show no significant correlation. In other words, the monsoon metric is correlated with EffCS in CIM, weakly correlated in CWAF, and not correlated at all in the other two regions. Even for CIM, some high-EffCS members project a smaller metric change than some of the low-med-EffCS members (Figure 2). Moreover, the spread across members of an individual model (with the same EffCS value) is comparable to the median difference between low-med- and high-EffCS models, even for the CIM region (Figure 2 and Table 2). These findings hold across different SSPs (Figures S2 and S5 and Tables S1–S4 in Supporting Information S1). In particular, even fewer significant correlations for CIM (~58%) are found in SSP5-8.5 than in SSP3-7.0, while in SSP2-4.5 no more than ~30% significant correlations are found for any region.

Table 2

Difference in Median Impact Metric Values Between High-EffCS and Low-Med-EffCS Models, Compared With the Spread Across Members for Individual Low-Med-EffCS Models

Region	Difference between high- and low-med-EffCS medians (absolute value)	Average spread in low-med-EffCS models (absolute value)	Largest spread in low-med-EffCS models (absolute value)
Flood			
Core West African Monsoon (CWAF)	126.01 mm	161.10 mm	219.68 mm
Core Indian Monsoon (CIM)	340.63 mm	229.21 mm	550.95 mm
North Central America (NCA)	25.00 mm	132.45 mm	275.63 mm
South Central America (SCA)	297.12 mm	230.05 mm	805.25 mm
Drought			
East Asia (EAS)	0.044692	0.079403	0.118613
Central North America (CNA)	0.0056226	0.071512	0.127481
Mediterranean (MED)	0.0074561	0.075394	0.118434
Fire			
Amazon (AMZ)	485 days	134 days	247 days
Australia (AUS)	101 days	256 days	485 days
Western North America (WNA)	122 days	145 days	230 days

A study (Jin et al., 2020) evaluating the quality of simulated present-day monsoons (1979–2014) in 24 CMIP6 models found the 10 best performing models to have EffCS values between 2.5 and 5.5K; the five best models are UKESM1-0-LL (EffCS 5.36K), CESM2 (5.16K), CESM2-WACCM (4.68K), MIROC6 (2.6K) and NorESM2-MM (2.49K). The spread in EffCS across the five models suggests little relationship between the quality of present-day simulated monsoon and model EffCS. The similarity of performance for CESM2 and NorESM2-MM is particularly interesting as these models share largely the same atmosphere and land models, but have very different ocean models. Their EffCS values, derived from the CMIP6 Abrupt-4xCO₂ experiment, are radically different because of differences in ocean heat uptake in the Southern Ocean (Gjermundsen et al., 2021). A comparably accurate simulation of the present-day monsoon in these two models suggests their common atmosphere and land models are likely most important, while processes responsible for the radically different EffCS in the two models are of secondary importance with respect to representing the present-day monsoon.

Our results suggest the relationship between the monsoon metric and EffCS is weakened by other drivers. Aerosols are the primary non-EffCS controls on monsoon precipitation (Wilcox et al., 2020). Increased aerosol loading, particularly of non-absorbing aerosols such as sulphate, increases atmospheric solar reflectivity close to the emission source (Ramanathan et al., 2001), cooling the land surface more than the adjacent ocean, weakening the land-ocean thermal gradient that drives the monsoon. Cooling, from increased solar reflection, also decreases atmospheric water vapor. Both changes act to decrease monsoon precipitation. In addition, absorbing aerosols such as black carbon, increase solar heating of the lower atmosphere, predominantly over land. This will increase atmospheric stability and reduce convective activity (Ramanathan et al., 2001). This heating will also tend to strengthen the monsoon surface pressure gradient, potentially enhancing circulation strength (Fang et al., 2023), highlighting the complex and competing role aerosols play in forcing the South Asian monsoon. Modeling studies (Ayantika et al., 2021; Bollasina et al., 2011) suggest past observed (decreasing) trends in mean South Asian monsoon precipitation arise from the impact of anthropogenic aerosol emissions (decreasing precipitation) outweighing the impact of CO₂-forced warming (increasing precipitation). One study (Zhao et al., 2019) shows that variations in regional aerosols are up to 4 times more efficient in

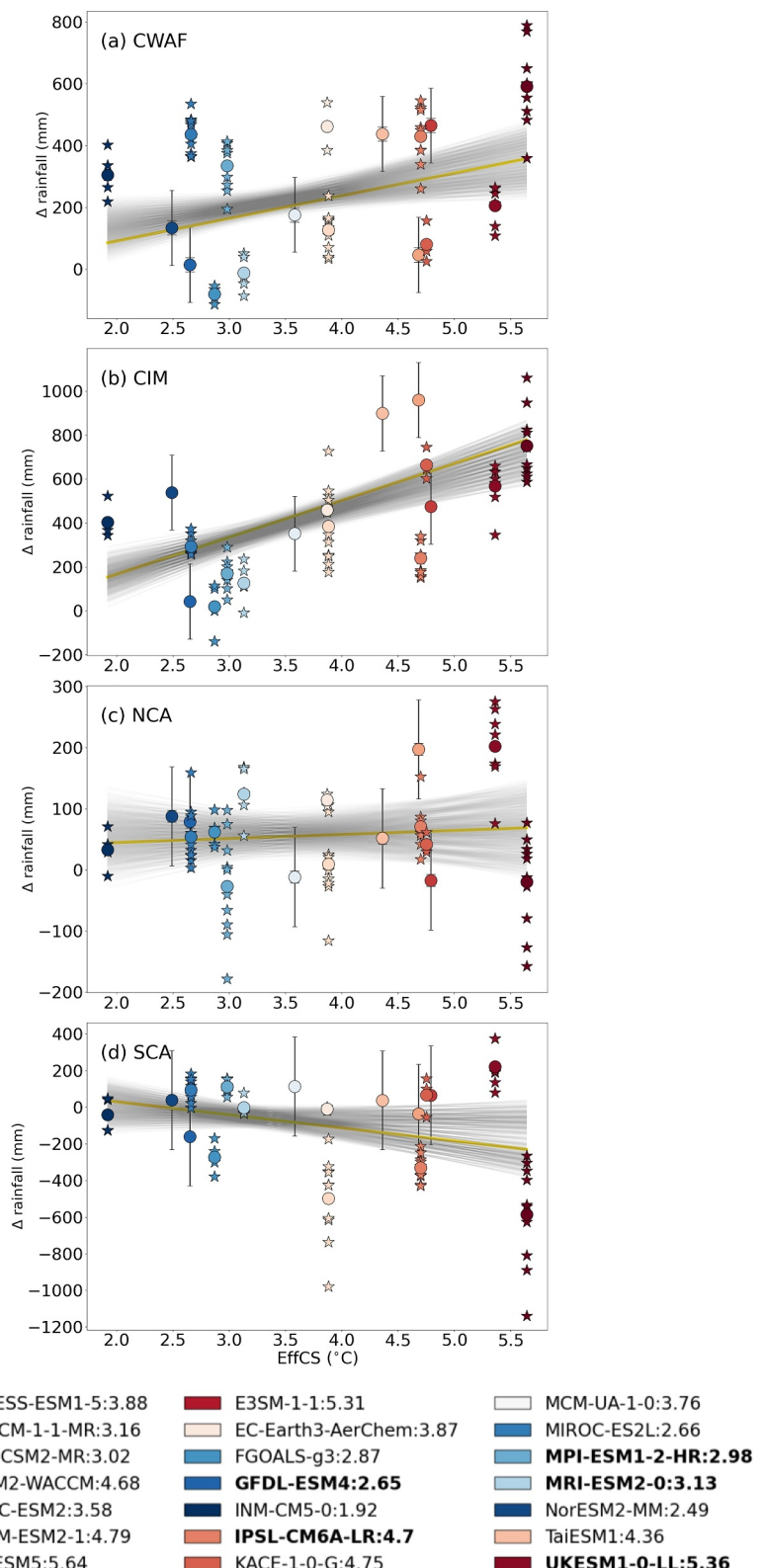


Figure 2.

impacting South Asian monsoon rainfall than equivalent variations in atmospheric CO₂, with extreme precipitation intensities particularly impacted by aerosols.

Aerosols also play an important role in the West African monsoon (Hirasawa et al., 2020, 2022). During the 1950s–1970s, increasing North American (NA) aerosols induced a drying effect on Sahel rainfall. This effect was mediated by slower sea surface temperature (SST) responses to regional aerosol emission trends across the globe, with cooling of the tropical west Pacific driving a remote wetting signal over the Sahel and cooling of the tropical Atlantic inducing a drying signal. The combination of these three drivers saw Sahel rainfall decline over the 1950s–1970s. During the 1970s–2000s increasing African aerosol emissions drove a direct drying over the Sahel. This local effect was balanced by a wetting signal associated with Atlantic warming (due to decreasing NA aerosols), amplified by a continued remote wetting signal from the west Pacific. The net result was an increase in precipitation over this period.

For both the South Asian and West African monsoon, trends in regional aerosols have significant and competing impacts on precipitation. These impacts are not considered in the calculation of EffCS, which results solely from an increase in atmospheric CO₂ within a constant pre-industrial aerosol state. Any relationship between model EffCS and projected changes in monsoon precipitation, derived from more realistic future emission scenarios that include time-varying CO₂, aerosol, and aerosol precursor emissions, will therefore be significantly weakened because of the confounding influence of aerosols.

Monsoons are also influenced by remote atmospheric teleconnections. The South Asian monsoon is influenced by the El Niño-Southern Oscillation (ENSO) SST variability (Webster et al., 1998). The West African monsoon is influenced by multi-decadal Atlantic SST variability (Biasutti, 2013) and by atmospheric subsidence induced over the Sahara as a remote response to the South Asian monsoon (Rodwell & Hoskins, 1996). In addition, the NCA and SCA monsoons are heavily impacted by ENSO variability and by anomalous subsidence forced by the West African and South Asian monsoons (He et al., 2020). These impacts are sufficiently large that neither the NCA nor SCA monsoon metric show any relationship with EffCS across the CMIP6 ensemble.

In addition to regional aerosols and atmospheric teleconnections, monsoon precipitation also depends on local convection and atmospheric water availability, which themselves are sensitive to model representation of local land-vegetation-atmosphere interactions (Chakraborty et al., 2023), the Himalayan snowpack (for CIM), and meso-convective-scale processes generally not resolved in ESMs (Fitzpatrick et al., 2020). The extent to which ESMs capture these mechanisms has little relation with EffCS. For reliable estimates of future monsoon rainfall, in addition to simulating the impact of increasing CO₂ (and other greenhouse gases), models also need to accurately simulate the impact of regional aerosol emissions, remote drivers of monsoon variability and small-scale, local processes and process interactions. All of these demands significantly weaken any link between model EffCS and projected changes in monsoon precipitation when realistic emission and land-use scenarios are used.

4.2. Drought

Figure 3 shows the projected change in the number of drought events per year as a function of EffCS. In almost all projections, the number of droughts increases in the future, consistent with earlier studies using CMIP5 (Dai, 2013) and CMIP6 data (Balting et al., 2021; Cook et al., 2020). However, for all regions we fail to find a significant correlation between the drought change metric and EffCS for the first variant, and for all but one region for the highest ensemble member of the low-EffCS models (Table 3). More precisely, only ~4% of all possible ensemble member combinations exhibit a statistically significant correlation across all models. Furthermore, the difference in the median metric between high- and low-med-EffCS models is always considerably smaller than

Figure 2. Change in area-averaged, total cumulative 5-day rainfall of the 20 most intense rainfall events per 20-year period, versus model effective climate sensitivities (EffCS) value. Change is calculated as 2081–2100 (under SSP3-7.0) minus 1995–2014. (a) Core West African monsoon region (CWAF), (b) Core Indian monsoon region (CIM), (c) North Central America (NCA), (d) South Central America (SCA). For each model, individual ensemble members are denoted by stars, and the ensemble mean value by a circle. Models with a single ensemble member include error bars indicating the largest (in black) and smallest (in gray, may be hidden behind model symbol) standard deviations as derived from all models with multiple ensemble members. The yellow line shows the best fit for the first (in some cases, only) ensemble member for each model. The gray area is formed from numerous individual lines each showing the best fit to a possible combination of one ensemble member from each model. The model EffCS value is mapped to color and the five model simulations that are used as input to many impact models (Lange & Büchner, 2021) are highlighted in bold (see legend).

Table 3

Significance of Correlation (at 95% Significance Level) Between Change in Impact Drivers and Effective Climate Sensitivities

Region	Number of low-med-EffCS members exceeding high-EffCS median (models contributing those members)	Percentage of statistically significant correlations in low-med-EffCS models	Percentage of significant correlations in all models	r1 ensemble member correlation	Highest ensemble member of low-med-EffCS models correlation
Flood					
Core West African Monsoon (CWAF)	13 (5)	0	3.90	Not significant	Not significant
Core Indian Monsoon (CIM)	2 (2)	4.69	77.78	Significant	Not Significant
North Central America (NCA)	18 (9)	0	0.15	Not significant	Not significant
South Central America (SCA)	39 (11)	0	0	Not significant	Not significant
Drought					
East Asia (EAS)	9 (4)	21.09	3.857	Not significant	Significant
Central North America (CNA)	21 (7)	0	4.248	Not significant	Not significant
Mediterranean (MED)	20 (8)	0	4.346	Not significant	Not significant
Fire					
Amazon (AMZ)	4 (2)	0	100	Significant	Not Significant
Australia (AUS)	12 (2)	6.25	32.71	Significant	Not significant
Western North America (WNA)	38 (8)	0	0	Not significant	Not significant

the mean of the spread across only low-med-EffCS members (Table 2). These results are confirmed by the analysis of different SSPs; the largest fraction of significant correlations, ~20%, is found under SSP5-8.5 for East Asia (Figures S3 and S6 and Tables S1–S4 in Supporting Information S1).

This is likely because changes in drought are forced by several climate drivers, with only one of these drivers being the magnitude of global warming. Local land warming, linked but not directly proportional to global mean warming, leads to increased evapotranspiration and vegetation water use, increasing drought risk, while higher atmospheric CO₂ counters this through increased plant water-use efficiency (Dai et al., 2018), making drought sensitive to local land-vegetation-atmosphere feedbacks. Many drought-prone regions today are located at the poleward edge of the subtropics, under the descending branch of the Hadley Cell, which induces persistent anticyclonic descending air, with dry conditions and high solar radiation. Future changes in regional drought will be highly sensitive to any systematic changes in the Hadley Cell. While observations indicate the Hadley cell has expanded poleward over recent decades (Staten et al., 2020) and models suggest a continued expansion in the future (Grise & Davis, 2020), zonal asymmetries in ocean warming, as well as differential responses between the ocean and land, lead to regional variations in projected Hadley cell expansion (Ma et al., 2018) and its impact on drought.

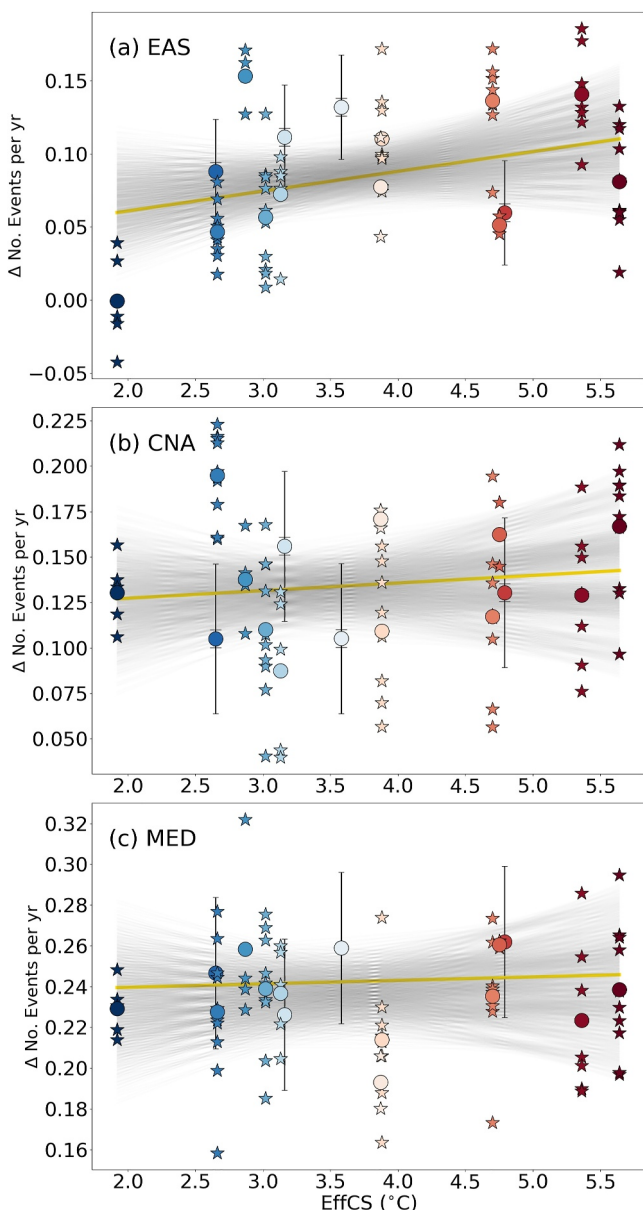


Figure 3. As Figure 2 but for change in the number of extreme drought events per year. (a) East Asia (EAS), (b) Central North America (CNA), (c) Mediterranean (MED).

In addition, drought prone regions in the mid-latitudes are influenced by transient weather systems that propagate along the jet stream. Periodically, these systems are “blocked” by long-lived meanders in the jet (Woollings et al., 2018). Such blocking events are important drivers of drought (Liu et al., 2020; Perry, 1976). The frequency and duration of such blocking depends on the strength of the jet, with a weaker jet allowing more and longer meanders (blocking events) (Nakamura & Huang, 2018). The jet strength is controlled by the tropical to pole tropospheric temperature gradient, with a stronger gradient resulting in a stronger and more zonal jet and fewer blocking events. The zonal mean response to increasing GHGs is warming of the tropical mid to upper troposphere and warming constrained close to the surface in polar regions, particularly in the Northern Hemisphere. As a result, it is thought that the jet stream will both strengthen and move poleward in the future (Shaw, 2019). Such a response would decrease the number and intensity of blocking meanders and change their preferred location: poleward and, over the Eurasian sector, eastward (Kennedy et al., 2016), with important consequences for future regional drought. While models have improved in simulating blocking, significant biases remain, even in the latest CMIP6 models (Davini & D’Andrea, 2020). Nevertheless, models show a consistent reduction in future blocking events, with a poleward and eastward shift of the main centers of action, potentially countering the impact of Hadley Cell poleward expansion. In addition to these dynamical/circulation controls on regional drought, trends in regional aerosol emissions can also impact atmospheric circulation and drought (Chiang et al., 2021).

The competing impacts of increasing CO_2 , trends in aerosol emissions, changes in regional circulation features, such as atmospheric blocking and regional land-atmosphere interactions, all mean accurately simulating past and future drought is a challenge. CMIP6 models reproduce historical drought with reasonable accuracy (Balting et al., 2021; Yu et al., 2023), although no single model stands out as best (Papalexiou et al., 2021). Additionally, while thermodynamic factors are responsible for average changes in the hydrological cycle, variability across models is governed by the dynamical (circulation) response to warming (Elbaum et al., 2022). Based on our results, filtering models solely on EffCS is not justified for drought assessment.

4.3. Fire

Figure 4 shows that for almost all ensemble members, fire weather days are projected to increase in the future compared to today as a function of EffCS. However, in Figure 1, fire metric frequency distributions for high- and low-med-EffCS models show a high degree of overlap, particularly for AUS. Over AMZ there is a clear tendency for high-EffCS models to simulate a larger increase in the number of fire weather days, while over WNA the opposite is the case.

Considering the full CMIP6 ensemble, a statistically significant relationship between EffCS and our fire metric can be seen for AMZ (Figures 4a and Table 3). However, this relationship is heavily influenced by the very lowest and highest EffCS models that simulate the smallest and largest change in fire metric respectively, while models between these two extremes have a more nuanced and flatter relationship. For AUS, the relationship with EffCS is only partly significant (Table 2), and the largest increase in fire weather is simulated by the ACCESS model, which has an intermediate EffCS value (Figure 4b). We also find that the spread within and across the high-EffCS models is within the range of the low-med-EffCS set (Figures 1 and 4b), and therefore excluding them brings no clear benefit while reducing the sample size, or biasing the subsample, for impact studies. Similarly, the difference in behavior between high- and low-med-EffCS median values is smaller than the average spread across low-med-EffCS models in AUS (Table 2). For WNA, there is no significant correlation with EffCS (Figure 4c and

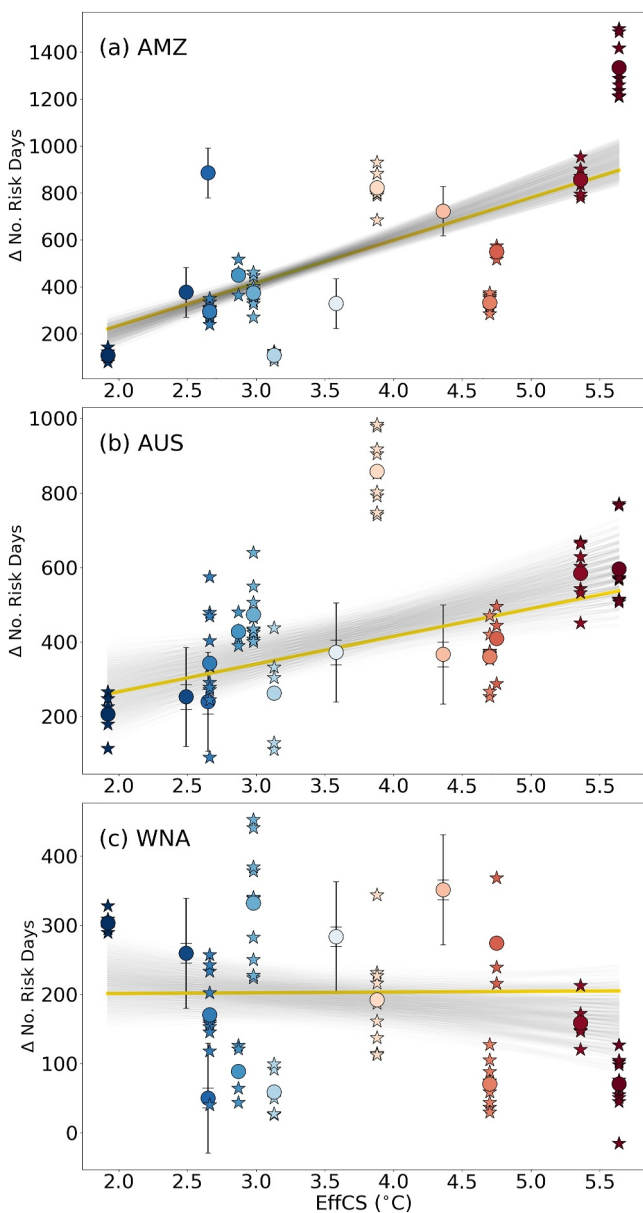


Figure 4. As Figure 2 but for change in the number of fire risk days per 20 year period. (a) Amazon (AMZ), (b) Australia (AUS), (c) Western North America (WNA).

5. Discussion and Conclusions

For 10 regions and three climate impact drivers of extreme monsoon rainfall, drought, and fire we find no universal correlation between projected changes in these drivers and EffCS. For some regions and drivers, a correlation does exist (e.g., AMZ fire or CIM monsoon rainfall), while for most there is no clear relationship. Where a correlation is identified, it is not straightforward to attribute future changes in our regional metric solely to EffCS, with many other factors also contributing. For all three drivers, even the sign of the correlation depends on the region. Furthermore, for all drought regions, the majority of monsoon flood, and fire regions, the spread in projected changes across the full CMIP6 ensemble, or often across a single model ensemble, is larger than, or of similar magnitude to, the difference in the median value of the metric between high- and low-med-EffCS models. Considering the variety of regions and drivers, this should not be a surprise. All three drivers are influenced by multiple factors. For a few regions and drivers EffCS may be the most important (though not the only) controlling

Table 3). Here, models with an EffCS around 3K project the largest increase, and the model with the highest EffCS (CanESM) projects the smallest change. Results from SSP2-4.5 and SSP5-8.5 confirm those from SSP3-7.0 (Figures S4 and S7 in Supporting Information S1): A statistically significant relationship between EffCS and our fire metric is found for AMZ and partially for AUS, but not for WNA (Tables S2 and S4 in Supporting Information S1); and the difference between the median values of high- and low-med-EffCS sets is smaller than the average spread across low-med-EffCS models except for AMZ (Tables S1 and S3 in Supporting Information S1). As for SSP3-7.0, the relationship in AMZ is strongly influenced by the very highest EffCS model.

Wildfires pose a significant threat to communities and ecosystems. Climate influences fire through several mechanisms, such as fuel load, dryness of fuel from water deficit, heat, and spreading by winds. These factors make fire potentially sensitive to climate change, where higher temperatures or longer dry spells (Jain et al., 2021) can contribute to increased fire activity. Increased warming leads to higher evapotranspiration, which dries out fuels including vegetation, soils and litter, and fires are often linked with periods of drought. A strong relationship might be expected between projected changes in fire and EffCS, given that temperature is a key driver of fire weather. Yet our results for three fire-prone regions suggest EffCS is not the leading determinant of future change in fire. The results show a stronger relationship between EffCS and our fire metric in AMZ, where historic changes in fire regimes have been attributed to anthropogenic activity (Aragão et al., 2014; Silveira et al., 2022). Yet we find no relationship in WNA, despite already observed increases in present-day fire weather which have been attributed to climate change (Abatzoglou & Williams, 2016; Zhuang et al., 2021). In Australia, there has been some observed increase in fire weather (Jones et al., 2022) and fires may be becoming larger and more intense (Abram et al., 2021), although whether this is anthropogenically forced is less clear due to natural variability from the Indian Ocean Dipole and ENSO (Hope et al., 2018; Lewis et al., 2019). These results indicate that changes in regional fire weather are generally not directly related to EffCS. In reality, multiple interacting factors influence fire occurrence, not limited to temperature, but also fuel availability, dryness, natural fire ignition (e.g., by lightning), and ignition and suppression by humans (Forkel et al., 2017, 2019). Large scale modes of variability such as ENSO also influence fire weather from year-to-year, and warming of the Tropical North Atlantic Ocean has been associated with increased drought and fires in Amazonia (Marengo et al., 2018). As with floods and drought, an approach that is more nuanced than only focusing on EffCS is required before models can be excluded.

factor, but for most drivers and regions it is just one of many controls. While our results are contingent on the choice of region and driver studied, all regions are known hotspots for their respective impact. WNA, AMZ and AUS have experienced extreme recent wildfire years; CNA, MED and EAS strong droughts; and the South Asian monsoon major flood events in 2022 and 2023 ("Centre for Research on the Epidemiology of Disasters" 2021). Moreover, here we study the climatic drivers of regional impacts. Impact models themselves (as well as real-world societal impacts) are more complex, involving numerous interactions between climatic drivers, biogeophysical and human responses and subsequent societal impact. We therefore believe the results from impact models will be even less clearly related to EffCS than the climate impact drivers studied here.

Societal impacts of climate change often occur at small spatial scales. As scales decrease, uncertainty in the forced climate change signal increases, partly because natural climate variability also increases. It is therefore even more important that information sampling this uncertainty is not thrown away without good reason. Thresholds may exist that trigger societal impacts, considering a broad range of possible regional climate changes is therefore important for understanding the true risk to society. Rejecting ESM projections for regional impact assessment, based solely on EffCS, should therefore be avoided in the absence of additional motivation, especially because it risks ignoring large parts of the range of potential impacts (Cannon, 2024). It is important to check if there is a statistically significant relationship between the criterion used for model selection (e.g., EffCS) and the climate drivers of the impacts in question. If this is not the case, or only partially true, then other factors should be considered before rejecting, or weighting models (Lorenz et al., 2018; Massoud et al., 2023), as both strategies may end up underestimating uncertainty (Knutti, 2010). For three impact drivers, over several regions, other factors such as aerosol forcing, atmospheric circulation and teleconnection changes, as well as local atmosphere-land-vegetation interactions are often as important as EffCS for determining the projected change in a regional impact driver. For each driver, it is important to identify the main processes inducing significant change in the driver and carefully evaluate each model's representation of these processes. It is not sufficient to assume such regional responses simply scale with model EffCS, as they generally do not. As an example not covered in our study, variability in future streamflow ensemble projections has been found to variously increase, decrease, or remain unchanged when high-EffCS models are removed, depending on the region studied (Asenjan et al., 2023).

Our results emphasize the important role of internal (or natural) variability plays in changes in regional climate drivers and their resultant impacts. For most drivers we studied, the spread across a single model ensemble is often larger than the difference in the driver between high-EffCS and low-med-EffCS models. This is also true when a smaller subset of models is considered, for example, those selected for the ISIMIP3 activity (Figure S1 in Supporting Information S1). Sampling a sufficient range of plausible impacts, including possible extreme outcomes, requires impact model experiments sample the full range of plausible changes in regional climate drivers. When it is not practical to run an entire CMIP ensemble (including all model members) through an impact model, analysis of relevant climate impact drivers across the full multi-model ensemble can help inform the selection of ESMs, and model members, that both spans the range of plausible future change, and emphasizes the most likely outcomes.

Selecting ESMs for regional impact studies based solely on EffCS has little (often zero) justification. Without more careful consideration, any such reduced ensemble used for impact studies will be unnecessarily biased. In the worst case, this will lead to the exclusion of models with plausible estimates of regional impact drivers, and the impacts themselves, with negative consequences for the robustness of scientific support for decision-making.

Data Availability Statement

All data is available through the Earth System Grid Federation (ESGF) (Cinquini et al., 2014) and was downloaded and preprocessed using the open source software ESMValCore (Andela et al., 2023a) and ESMValTool (Andela et al., 2023b). Software developed to calculate the three impact metrics, perform statistical analyses and preprocessed data used to create the figures in this paper is in the process of being archived with the open source zenodo repository as (Swaminathan et al., 2024).

References

Abatzoglou, J. T., & Williams, A. P. (2016). Impact of anthropogenic climate change on wildfire across western US forests. *Proceedings of the National Academy of Sciences of the United States of America*, 113(42), 11770–11775. <https://doi.org/10.1073/pnas.1607171113>

Abram, N. J., Henley, B. J., Gupta, A. S., Lippmann, T. J. R., Clarke, H., Dowdy, A. J., & Sharples, J. J. (2021). Connections of climate change and variability to large and extreme forest fires in Southeast Australia. *Communications Earth & Environment*, 2(1), 1–17.

Andela, B., Broet, B., de Mora, L., Drost, N., Eyring, V., Koldunov, N., et al. (2023a). *ESMValCore* (v2.9.0). Zenodo. <https://doi.org/10.5281/zenodo.8112684>

Andela, B., Broet, B., de Mora, L., Drost, N., Eyring, V., Koldunov, N., et al. (2023b). *ESMValTool* (v2.9.0). Zenodo. <https://doi.org/10.5281/zenodo.1040890>

Andela, N., Morton, D. C., Giglio, L., Chen, Y., Werf, G. R., Kasibhatla, P. S., et al. (2017). A human-driven decline in global burned area. *Science*, 356(6345), 1356–1362. <https://doi.org/10.1126/science.aal4108>

Aragão, L. E. O. C., Poulter, B., Barlow, J. B., Anderson, L. O., Malhi, Y., Saatchi, S., et al. (2014). Environmental change and the carbon balance of Amazonian Forests. *Biological Reviews of the Cambridge Philosophical Society*, 89(4), 913–931. <https://doi.org/10.1111/brv.12088>

Asenjan, M. R., Brissette, F., Martel, J.-L., & Arsenault, R. (2023). Understanding the influence of “hot” models in climate impact studies: A hydrological perspective. *European Geosciences Union*, 27(23), 4355–4367. <https://doi.org/10.5194/hess-27-4355-2023>

Ayantika, D. C., Krishnan, R., Singh, M., Swapna, P., Sandeep, N., Prajesh, A. G., & Vellore, R. (2021). Understanding the combined effects of global warming and anthropogenic aerosol forcing on the South Asian monsoon. *Climate Dynamics*, 56(5), 1643–1662. <https://doi.org/10.1007/s00382-020-05551-5>

Balting, D. F., AghaKouchak, A., Lohmann, G., & Ionita, M. (2021). Northern hemisphere drought risk in a warming climate. *Npj Climate and Atmospheric Science*, 4(1), 1–13. <https://doi.org/10.1038/s41612-021-00218-2>

Beguería, S., Vicente, S., Latorre, B., & Reig, F. (2023). SPEI. Retrieved from <https://spei.csic.es/>

Beguería, S., Vicente-Serrano, S. M., Reig, F., & Latorre, B. (2014). Standardized precipitation evapotranspiration index (SPEI) revisited: Parameter fitting, evapotranspiration models, tools, datasets and drought monitoring. *International Journal of Climatology*, 34(10), 3001–3023. <https://doi.org/10.1002/joc.3887>

Biasutti, M. (2013). Forced Sahel rainfall trends in the CMIP5 archive. *Journal of Geophysical Research*, 118(4), 1613–1623. <https://doi.org/10.1002/jgrd.50206>

Bloch-Johnson, J., Rugenstein, M., Stolpe, M. B., Rohrschneider, T., Zheng, Y., & Gregory, J. M. (2021). Climate sensitivity increases under higher CO₂ levels due to feedback temperature dependence. *Geophysical Research Letters*, 48(4), 089074. <https://doi.org/10.1029/2020gl089074>

Bock, L., Lauer, A., Schlund, M., Barreiro, M., Bellouin, N., Jones, C., et al. (2020). Quantifying progress across different CMIP phases with the ESMValTool. *Journal of Geophysical Research*, 125(21). <https://doi.org/10.1029/2019jd032321>

Bollasina, M. A., Ming, Y., & Ramaswamy, V. (2011). Anthropogenic aerosols and the weakening of the South Asian summer monsoon. *Science*, 334(6055), 502–505. <https://doi.org/10.1126/science.1204994>

Boysen, L. R., Brovkin, V., Pongratz, J., Lawrence, D. M., Lawrence, P., Vuichard, N., et al. (2020). Global climate response to idealized deforestation in CMIP6 models. *Biogeosciences*, 17(22), 5615–5638. <https://doi.org/10.5194/bg-17-5615-2020>

Byrne, M. P., & O’Gorman, P. A. (2018). Trends in continental temperature and humidity directly linked to ocean warming. *Proceedings of the National Academy of Sciences of the United States of America*, 115(19), 4863–4868. <https://doi.org/10.1073/pnas.1722312115>

Cannon, A. J. (2024). The impact of “hot models” on a CMIP6 ensemble used by climate service providers in Canada: Do global constraints lead to appreciable differences in regional projections? *Journal of Climate*, 37(6), 2141–2154. <https://doi.org/10.1175/jcli-d-23-0459.1>

Caretta, M. A., Mukherji, A., Arfanuzzaman, M., Betts, R. A., Gelfan, A., Hirabayashi, Y., et al. (2022). Water. In D. C. Roberts, M. Tignor, E. S. Poloczanska, K. Mintenbeck, A. Alegria, S. L. M. Craig, et al. (Eds.), *Climate change 2022: Impacts, adaptation and vulnerability. Contribution of working group II to the Sixth assessment report of the intergovernmental panel on climate change* (pp. 551–712). Cambridge University Press. [H.-O. Pörtner]. <https://doi.org/10.1017/9781009325844.006>

Centre for Research on the Epidemiology of Disasters. (2021). Public EM-DAT platform. Retrieved from <https://public.emdat.be/>

Chakraborty, A., Samuel, J. B., & Paleri, A. (2023). Role of land–surface vegetation in the March of Indian monsoon onset isochrones in a coupled model. *Quarterly Journal of the Royal Meteorological Society*, 149(750), 115–132. <https://doi.org/10.1002/qj.4398>

Chapter 7: The Earth’s energy budget, climate feedbacks, and climate sensitivity. (2021). Open Access Victoria University of Wellington | Te Herenga Waka. <https://doi.org/10.25455/WGTN.16869671.V1>

Chiang, F., Mazdiyasni, O., & AghaKouchak, A. (2021). Evidence of anthropogenic impacts on global drought frequency, duration, and intensity. *Nature Communications*, 12(1), 2754. <https://doi.org/10.1038/s41467-021-22314-w>

Cinquini, L., Crichton, D., Mattmann, C., Harney, J., Shipman, G., Wang, F., et al. (2014). The Earth system grid federation: An open infrastructure for access to distributed geospatial data. *Future Generation Computer Systems*, 36, 400–417. <https://doi.org/10.1016/j.future.2013.07.002>

Cook, B. I., Mankin, J. S., Marvel, K., Williams, A. P., Smerdon, J. E., & Anchukaitis, K. J. (2020). Twenty-first century drought projections in the CMIP6 forcing scenarios. *Earth’s Future*, 8(6). <https://doi.org/10.1029/2019ef001461>

Dai, A. (2013). Increasing drought under global warming in observations and models. *Nature Climate Change*, 3(1), 52–58. <https://doi.org/10.1038/nclimate1633>

Dai, A., Zhao, T., & Chen, J. (2018). Climate change and drought: A precipitation and evaporation perspective. *Current Climate Change Reports*, 4(3), 301–312. <https://doi.org/10.1007/s40641-018-0101-6>

Davini, P., & D’Andrea, F. (2020). From CMIP3 to CMIP6: Northern hemisphere atmospheric blocking simulation in present and future climate. *Journal of Climate*, 33(23), 10021–10038. <https://doi.org/10.1175/jcli-d-19-0862.1>

Elbaum, E., Garfinkel, C. I., Adam, O., Morin, E., Rostkier-Edelstein, D., & Dayan, U. (2022). Uncertainty in projected changes in precipitation minus evaporation: Dominant role of dynamic circulation changes and weak role for thermodynamic changes. *Geophysical Research Letters*, 49(12). <https://doi.org/10.1029/2022gl097725>

Eyring, V., Bony, S., Meehl, G. A., Senior, C. A., Stevens, B., Stouffer, R. J., & Taylor, K. E. (2016). Overview of the Coupled Model Inter-comparison Project Phase 6 (CMIP6) experimental design and organization. *Geoscientific Model Development*, 9(5), 1937–1958. <https://doi.org/10.5194/gmd-9-1937-2016>

Eyring, V., Cox, P. M., Flato, G. M., Gleckler, P. J., Abramowitz, G., Caldwell, P., et al. (2019). Taking climate model evaluation to the next level. *Nature Climate Change*, 9(2), 102–110. <https://doi.org/10.1038/s41558-018-0355-y>

Eyring, V., Gillett, N. P., Achuta Rao, K. M., Barimalala, R., Barreiro Parrillo, M., Bellouin, N., & Cassou, C. (2021). Human influence on the climate system. In V. Masson-Delmotte, P. Zhai, A. Pirani, S. L. Connors, C. Péan, & S. Berger (Eds.), *Climate Change 2021: The Physical Science Basis: Working Group I Contribution to the Sixth Assessment Report of the Intergovernmental Panel on Climate Change* (pp. 423–552). Cambridge University Press. <https://doi.org/10.1017/9781009157896.005>

Fang, C., Haywood, J. M., Liang, J., Johnson, B. T., Chen, Y., & Zhu, B. (2023). Impacts of reducing scattering and absorbing aerosols on the temporal extent and intensity of South Asian summer monsoon and East Asian summer monsoon. *Atmospheric Chemistry and Physics*, 23(14), 8341–8368. <https://doi.org/10.5194/acp-23-8341-2023>

Fitzpatrick, R. G. J., Parker, D. J., Marsham, J. H., Rowell, D. P., Guichard, F. M., Taylor, C. M., et al. (2020). What drives the intensification of mesoscale convective systems over the West African Sahel under climate change? *Journal of Climate*, 33(8), 3151–3172. <https://doi.org/10.1175/jcli-d-19-0380.1>

Forkel, M., Andela, N., Harrison, S. P., Lasslop, G., Marle, M., Chuvieco, E., et al. (2019). Emergent relationships with respect to burned area in global satellite observations and fire-enabled vegetation models. *Biogeosciences*, 16(1), 57–76. <https://doi.org/10.5194/bg-16-57-2019>

Forkel, M., Dorigo, W., Lasslop, G., Teubner, I., Chuvieco, E., & Thonicke, K. (2017). A data-driven approach to identify controls on global fire activity from satellite and climate observations (SOFIA V1). *Geoscientific Model Development*, 10(12), 4443–4476. <https://doi.org/10.5194/gmd-10-4443-2017>

Forster, P., Storelvmo, T., Armour, K., Collins, W., Dufresne, J.-L., Frame, D., et al. (2021). The Earth's Energy Budget, Climate Feedbacks, and Climate Sensitivity. In V. Masson-Delmotte, P. Zhai, A. Pirani, S. L. Connors, C. Péan, S. Berger, et al. (Eds.), *Climate Change 2021: The Physical Science Basis. Contribution of Working Group I to the Sixth Assessment Report of the Intergovernmental Panel on Climate Change* (pp. 923–1054). Cambridge University Press. <https://doi.org/10.1017/9781009157896.009>

Frieler, K., Lange, S., Piontek, F., Reyer, C. P. O., Schewe, J., Warszawski, L., et al. (2017). Assessing the impacts of 1.5°C global warming – Simulation protocol of the inter-sectoral impact model intercomparison project (ISIMIP2b). *Geoscientific Model Development*, 10(12), 4321–4345. <https://doi.org/10.5194/gmd-10-4321-2017>

Gjermundsen, A., Nummelin, A., Olivie, D., Bentsen, M., Selander, Ø., & Schulz, M. (2021). Shutdown of Southern Ocean convection controls long-term greenhouse gas-induced warming. *Nature Geoscience*, 14(10), 724–731. <https://doi.org/10.1038/s41561-021-00825-x>

Gregory, J. M., Ingram, W. J., Palmer, M. A., Jones, G. S., Stott, P. A., Thorpe, R. B., et al. (2004). A new method for diagnosing radiative forcing and climate sensitivity. *Geophysical Research Letters*, 31(3). <https://doi.org/10.1029/2003gl018747>

Grise, K. M., & Davis, S. M. (2020). Hadley cell expansion in CMIP6 models. *Atmospheric Chemistry and Physics*, 20(9), 5249–5268. <https://doi.org/10.5194/acp-20-5249-2020>

Hargreaves, G. H., & Samani, Z. A. (1985). Reference crop evapotranspiration from temperature. *Applied Engineering in Agriculture*, 1(2), 96–99. <https://doi.org/10.13031/2013.26773>

Hausfather, Z., Marvel, K., Schmidt, G. A., Nielsen-Gammon, J. W., & Zelinka, M. (2022). Climate simulations: Recognize the ‘hot model’ problem. *Nature*, 605(7908), 26–29. <https://doi.org/10.1038/d41586-022-01192-2>

He, C., Li, T., & Zhou, W. (2020). Drier North American monsoon in contrast to Asian–African monsoon under global warming. *Journal of Climate*, 33(22), 9801–9816. <https://doi.org/10.1175/jcli-d-20-0189.1>

Held, I. M., & Soden, B. J. (2006). Robust responses of the hydrological cycle to global warming. *Journal of Climate*, 19(21), 5686–5699. <https://doi.org/10.1175/jcli3990.1>

Hirasawa, H., Kushner, P. J., Sigmond, M., Fyfe, J., & Deser, C. (2020). Anthropogenic aerosols dominate forced multidecadal Sahel precipitation change through distinct atmospheric and oceanic drivers. *Journal of Climate*, 33(23), 10187–10204. <https://doi.org/10.1175/jcli-d-19-0829.1>

Hirasawa, H., Kushner, P. J., Sigmond, M., Fyfe, J., & Deser, C. (2022). Evolving Sahel rainfall response to anthropogenic aerosols driven by shifting regional oceanic and emission influences. *Journal of Climate*, 35(11), 3181–3193. <https://doi.org/10.1175/jcli-d-21-0795.1>

Hope, P., Black, M. T., Lim, E.-P., Dowdy, A., Wang, G., Fawcett, R. J. B., & Pepler, A. S. (2018). On determining the impact of increasing atmospheric CO₂ on the record fire weather in eastern Australia in February 2017. *Bulletin of the American Meteorological Society*, 100(1), 111–117. <https://doi.org/10.1175/bams-d-18-0135.1>

IPCC. (2022). Summary for Policymakers. In H.-O. Pörtner, D. C. Roberts, E. S. Poloczanska, K. Mintenbeck, M. Tignor, A. Alegria, et al. (Eds.), *Climate Change 2022: Impacts, Adaptation, and Vulnerability. Contribution of Working Group II to the Sixth Assessment Report of the Intergovernmental Panel on Climate Change* (pp. 3–33). Cambridge University Press. <https://doi.org/10.1017/9781009325844.001>

Iturbide, M., Gutiérrez, J. M., Alves, L. M., Bedia, J., Cerezo-Mota, R., Cimadevilla, E., et al. (2020). An update of IPCC climate reference regions for subcontinental analysis of climate model data: Definition and aggregated datasets. *Earth System Science Data*, 12(4), 2959–2970. <https://doi.org/10.5194/essd-12-2959-2020>

Jain, P., Castellanos-Acuna, D., Coogan, S. C. P., Abatzoglou, J. T., & Flannigan, M. D. (2021). Observed increases in extreme fire weather driven by atmospheric humidity and temperature. *Nature Climate Change*, 12(1), 63–70. <https://doi.org/10.1038/s41558-021-01224-1>

Jin, C., Wang, B., & Liu, J. (2020). Future changes and controlling factors of the eight regional monsoons projected by CMIP6 models. *Journal of Climate*, 33(21), 9307–9326. <https://doi.org/10.1175/jcli-d-20-0236.1>

Johnston, F. H., Borchers-Arriagada, N., Morgan, G. G., Jalaludin, B., Palmer, A. J., Williamson, G. J., & Bowman, D. M. J. S. (2021). Unprecedented health costs of smoke-related PM2.5 from the 2019–20 Australian megafires. *Nature Sustainability*, 4(1), 42–47. <https://doi.org/10.1038/s41893-020-00610-5>

Jones, M. W., Abatzoglou, J. T., Veraverbeke, S., Andela, N., Lasslop, G., Forkel, M., et al. (2022). Global and regional trends and drivers of fire under climate change. *Reviews of Geophysics*, 60(3). <https://doi.org/10.1029/2020rg000726>

Kennedy, D., Parker, T., Woollings, T., Harvey, B., & Shaffrey, L. (2016). The response of high-impact blocking weather systems to climate change. *Geophysical Research Letters*, 43(13), 7250–7258. <https://doi.org/10.1002/2016gl069725>

Knutti, R. (2010). The end of model democracy? An editorial comment. *Climatic Change*, 102(3), 395–404. <https://doi.org/10.1007/s10584-010-9800-2>

Lange, S., & Büchner, M. (2021). ISIMIP3b bias-adjusted atmospheric climate input data. *ISIMIP Repository*. <https://doi.org/10.48364/ISIMIP.842396.1>

Lasslop, G., Coppola, A. I., Voulgarakis, A., Yue, C., & Veraverbeke, S. (2019). Influence of fire on the carbon cycle and climate. *Current Climate Change Reports*, 5(2), 112–123. <https://doi.org/10.1007/s40641-019-00128-9>

Lawson & Armitage. (2008). Weather guide for the Canadian forest fire danger rating system. Retrieved from <https://www.frames.gov/catalog/6720>

Lee, J.-Y., Marotzke, J., Bala, G., Cao, L., Corti, S., Dunne, J. P., et al. (2021). Future global climate: Scenario-based projections and near-term information. In V. Masson-Delmotte, P. Zhai, A. Pirani, S. L. Connors, C. Péan, S. Berger, et al. (Eds.), *Climate Change 2021: The Physical Science Basis. Contribution of Working Group I to the Sixth Assessment Report of the Intergovernmental Panel on Climate Change* (pp. 553–672). Cambridge University Press. <https://doi.org/10.1017/9781009157896.006>

Lewis, S. C., Blake, S. A. P., Trewin, B., Black, M. T., Dowdy, A. J., Perkins-Kirkpatrick, S. E., et al. (2019). Deconstructing factors contributing to the 2018 fire weather in Queensland, Australia. *Bulletin of the American Meteorological Society*, 101(1), 115–122. <https://doi.org/10.1175/bams-d-19-0144.1>

Li, F., Song, X., Harrison, S. P., Marlon, J. R., Zhongda Lin, L. R. L., Schwinger, J., et al. (2024). Evaluation of global fire simulations in CMIP6 Earth System Models. <https://doi.org/10.5194/gmd-2024-85>

Liu, X., He, B., Guo, L., Huang, L., & Chen, D. (2020). Similarities and differences in the mechanisms causing the European summer heatwaves in 2003, 2010, and 2018. *Earth's Future*, 8(4). <https://doi.org/10.1029/2019ef001386>

Lorenz, R., Herger, N., Sedláček, J., Eyring, V., Fischer, E. M., & Knutti, R. (2018). Prospects and caveats of weighting climate models for summer maximum temperature projections over North America. *Journal of Geophysical Research*, 123(9), 4509–4526. <https://doi.org/10.1029/2017jd027992>

Ma, J., Chadwick, R., Seo, K.-H., Dong, C., Huang, G., Foltz, G. R., & Jiang, J. H. (2018). Responses of the tropical atmospheric circulation to climate change and connection to the hydrological cycle. *Annual Review of Earth and Planetary Sciences*, 46(1), 549–580. <https://doi.org/10.1146/annurev-earth-082517-010102>

Marengo, J. A., Souza, C. M., Jr., Thonicke, K., Burton, C., Halladay, K., Betts, R. A., et al. (2018). Changes in climate and land use over the Amazon region: Current and future variability and trends. *Frontiers of Earth Science*, 6. <https://doi.org/10.3389/feart.2018.00228>

Martin, E. R. (2018). Future projections of global pluvial and drought event characteristics. *Geophysical Research Letters*, 45(21), 11913–11920. <https://doi.org/10.1029/2018gl079807>

Massoud, E. C., Lee, H. K., Terando, A., & Wehner, M. (2023). Bayesian weighting of climate models based on climate sensitivity. *Communications Earth & Environment*, 4(1), 1–8. <https://doi.org/10.1038/s43247-023-01009-8>

Nakamura, N., & Huang, C. S. Y. (2018). Atmospheric blocking as a traffic jam in the jet stream. *Science*, 361(6397), 42–47. <https://doi.org/10.1126/science.aat0721>

O'Neill, B. C., Tebaldi, C., Vuuren, D. P., Eyring, V., Friedlingstein, P., Hurtt, G., et al. (2016). The scenario model intercomparison project (ScenarioMIP) for CMIP6. *Geoscientific Model Development*, 9(9), 3461–3482. <https://doi.org/10.5194/gmd-9-3461-2016>

Palmer, T. E., McSweeney, C. F., Booth, B. B., Priestley, M. D. K., Davini, P., Brunner, L., et al. (2023). Performance-based sub-selection of CMIP6 models for impact assessments in Europe. *Earth System Dynamics*, 14(2), 457–483. <https://doi.org/10.5194/esd-14-457-2023>

Papalexiou, S. M., Rajulapati, C. R., Andreidis, K. M., Foufoula-Georgiou, E., Clark, M. P., & Trenberth, K. E. (2021). Probabilistic evaluation of drought in CMIP6 simulations. *Earth's Future*, 9(10), 002150. <https://doi.org/10.1029/2021ef002150>

Parmesan, C., Morecroft, M. D., Trisurat, Y., Adrian, R., Anshari, G. Z., Arneth, A., et al. (2022). Terrestrial and Freshwater Ecosystems and Their Services. In H.-O. Pörtner, D. C. Roberts, M. Tignor, E. S. Poloczanska, K. Mintenbeck, A. Alegria, et al. (Eds.), *Climate Change 2022: Impacts, Adaptation and Vulnerability. Contribution of Working Group II to the Sixth Assessment Report of the Intergovernmental Panel on Climate Change* (pp. 197–377). Cambridge University Press. <https://doi.org/10.1017/9781009325844.004>

Perry, A. H. (1976). The long drought of 1975–76. *Weather*, 31(10), 328–336. <https://doi.org/10.1002/j.1477-8696.1976.tb07448.x>

Pullabhotla, H. K., Zahid, M., Heft-Neal, S., Rathi, V., & Burke, M. (2023). Global biomass fires and infant mortality. *Proceedings of the National Academy of Sciences of the United States of America*, 120(23), 2218210120. <https://doi.org/10.1073/pnas.2218210120>

Ramanathan, V., Crutzen, P. J., Kiehl, J. T., & Rosenfeld, D. (2001). Aerosols, climate, and the hydrological cycle. *Science*, 294(5549), 2119–2124. <https://doi.org/10.1126/science.1064034>

Ranasinghe, R., Ruane, A. C., Vautard, R., Arnell, N., Coppola, E., Cruz, F. A., et al. (2021). Climate Change Information for Regional Impact and for Risk Assessment. In V. Masson-Delmotte, P. Zhai, A. Pirani, S. L. Connors, C. Péan, S. Berger, et al. (Eds.), *Climate Change 2021: The Physical Science Basis. Contribution of Working Group I to the Sixth Assessment Report of the Intergovernmental Panel on Climate Change* (pp. 1767–1926). Cambridge University Press. <https://doi.org/10.1017/9781009157896.014>

Riahi, K., van Vuuren, D. P., Kriegler, E., Edmonds, J., O'Neill, B. C., Fujimori, S., Bauer, N., et al. (2017). The shared socioeconomic pathways and their energy, land use, and greenhouse gas emissions implications: An overview. *Global Environmental Change*, 42, 153–168. <https://doi.org/10.1016/j.gloenvcha.2016.05.009>

Ribes, A., Boé, J., Qasmi, S., Dubuisson, B., Douville, H., & Terray, L. (2022). An updated assessment of past and future warming over France based on a regional observational constraint. *Earth System Dynamics*, 13(4), 1397–1415. <https://doi.org/10.5194/esd-13-1397-2022>

Ribes, A., Qasmi, S., & Gillett, N. P. (2021). Making climate projections conditional on historical observations. *Science Advances*, 7(4). <https://doi.org/10.1126/sciadv.abc0671>

Righi, M., Andela, B., Eyring, V., Lauer, A., Predoi, V., Schlund, M., et al. (2020). Earth system model evaluation tool (ESMValTool) v2.0 – Technical overview. *Geoscientific Model Development*, 13(3), 1179–1199. <https://doi.org/10.5194/gmd-13-1179-2020>

Rodwell, M. J., & Hoskins, B. J. (1996). Monsoons and the dynamics of deserts. *Quarterly Journal of the Royal Meteorological Society*, 122(534), 1385–1404. <https://doi.org/10.1256/smsqj.53407>

Ruane, A. C., Vautard, R., Ranasinghe, R., Sillmann, J., Coppola, E., Arnell, N., et al. (2022). The climatic impact–driver framework for assessment of risk–relevant climate information. *Earth's Future*, 10(11), 002803. <https://doi.org/10.1029/2022ef002803>

Samset, B. H., Myhre, G., Forster, P. M., Hodnebrog, Ø., Andrews, T., Faluvegi, G., et al. (2016). Fast and slow precipitation responses to individual climate forcers: A PDRMIP multimodel study. *Geophysical Research Letters*, 43(6), 2782–2791. <https://doi.org/10.1002/2016GL068064>

Shaw, T. A. (2019). Mechanisms of future predicted changes in the zonal mean mid–latitude circulation. *Current Climate Change Reports*, 5(4), 345–357. <https://doi.org/10.1007/s40641-019-00145-8>

Silveira, M. V. F., Silva-Junior, C. H. L., Anderson, L. O., & Aragão, L. E. O. C. (2022). Amazon fires in the 21st century: The year of 2020 in evidence. *Global Ecology and Biogeography: A Journal of Macroecology*, 31(10), 2026–2040. <https://doi.org/10.1111/geb.13577>

Speizer, S., Raymond, C., Ivanovich, C., & Horton, R. M. (2022). Concentrated and intensifying humid heat extremes in the IPCC AR6 regions. *Geophysical Research Letters*, 49(5). <https://doi.org/10.1029/2021gl097261>

Staten, P. W., Grise, K. M., Davis, S. M., Karnauskas, K. B., Waugh, D. W., Maycock, A. C., et al. (2020). Tropical widening: From global variations to regional impacts. *Bulletin of the American Meteorological Society*, 101(6), 897–904. <https://doi.org/10.1175/bams-d-19-0047.1>

Swaminathan, R., Walton, J., & Zimmerman, K. (2024). Data and analysis and plotting scripts for Swaminathan et al Regional Impacts Poorly Constrained by Climate Sensitivity [Dataset]. Zenodo. <https://doi.org/10.5281/zenodo.10533860>

van Wagner, C. E. (1987). *Development and structure of the Canadian Forest Fire Weather Index System* (Forestry Technical Report No. 35, p. 37). Canadian Forest Service, Petawawa National Forestry Institute.

Vicente-Serrano, S. M., Beguería, S., & López-Moreno, J. I. (2010). A multiscalar drought index sensitive to global warming: The standardized precipitation evapotranspiration index. *Journal of Climate*, 23(7), 1696–1718. <https://doi.org/10.1175/2009jcli2909.1>

Wang, B., Jin, C., & Liu, J. (2020). Understanding future change of global monsoons projected by CMIP6 models. *Journal of Climate*, 33(15), 6471–6489. <https://doi.org/10.1175/jcli-d-19-0993.1>

Wang, Y., & Lewis, D. J. (2024). Wildfires and climate change have lowered the economic value of western U.S. Forests by altering risk expectations. *Journal of Environmental Economics and Management*, 123(January), 102894. <https://doi.org/10.1016/j.jeem.2023.102894>

Webster, P. J., Magaña, V. O., Palmer, T. N., Shukla, J., Tomas, R. A., Yanai, M., & Yasunari, T. (1998). Monsoons: Processes, predictability, and the prospects for prediction. *Journal of Geophysical Research*, 103(C7), 14451–14510. <https://doi.org/10.1029/97JC02719>

Wilcox, L. J., Liu, Z., Samset, B. H., Hawkins, E., Lund, M. T., Nordling, K., et al. (2020). Accelerated increases in global and Asian summer monsoon precipitation from future aerosol reductions. *Atmospheric Chemistry and Physics*, 20(20), 11955–11977. <https://doi.org/10.5194/acp-20-11955-2020>

Wood, R. A., Crucifix, M., Lenton, T. M., Mach, K. J., Moore, C., New, M., et al. (2023). A climate science toolkit for high impact–low likelihood climate risks. *Earth's Future*, 11(4). <https://doi.org/10.1029/2022ef003369>

Woollings, T., Barriopedro, D., Methven, J., Son, S.–W., Martius, O., Harvey, B., et al. (2018). Blocking and its response to climate change. *Current Climate Change Reports*, 4(3), 287–300. <https://doi.org/10.1007/s40641-018-0108-z>

Wu, M., Nikulin, G., Kjellström, E., Belušić, D., Jones, C., & Lindstedt, D. (2020). The impact of regional climate model formulation and resolution on simulated precipitation in Africa. *Earth System Dynamics*, 11(2), 377–394. <https://doi.org/10.5194/esd-11-377-2020>

Yu, X., Zhang, L., Zhou, T., & Zheng, J. (2023). Assessing the performance of CMIP6 models in simulating droughts across global drylands. *Advances in Atmospheric Sciences*, 41(2), 193–208. <https://doi.org/10.1007/s00376-023-2278-4>

Zelinka, M. D., Myers, T. A., McCoy, D. T., Po-Chedley, S., Caldwell, P. M., Ceppi, P., et al. (2020). Causes of higher climate sensitivity in CMIP6 models. *Geophysical Research Letters*, 47(1). <https://doi.org/10.1029/2019gl085782>

Zhao, A. D., Stevenson, D. S., & Bollasina, M. A. (2019). The role of anthropogenic aerosols in future precipitation extremes over the Asian monsoon region. *Climate Dynamics*, 52(9), 6257–6278. <https://doi.org/10.1007/s00382-018-4514-7>

Zhuang, Y., Fu, R., Santer, B. D., Dickinson, R. E., & Hall, A. (2021). Quantifying contributions of natural variability and anthropogenic forcings on increased fire weather risk over the western United States. *Proceedings of the National Academy of Sciences of the United States of America*, 118, 45. <https://doi.org/10.1073/pnas.2111875118>